LBL-11929
Preprint

Lawrence Berkeley Laboratory
UNIVERSITY OF CALIFORNIA

Materials & Molecular
Research Division

Submitted to Metallurgical Transactions

EFFECT OF VANADIUM ON STRUCTURE-PROPERTY RELATIONS OF DUAL PHASE Fe/Mn/Si/0.1C STEELS

Alvin Nakagawa, J.Y. Koo, and G. Thomas

March 1981

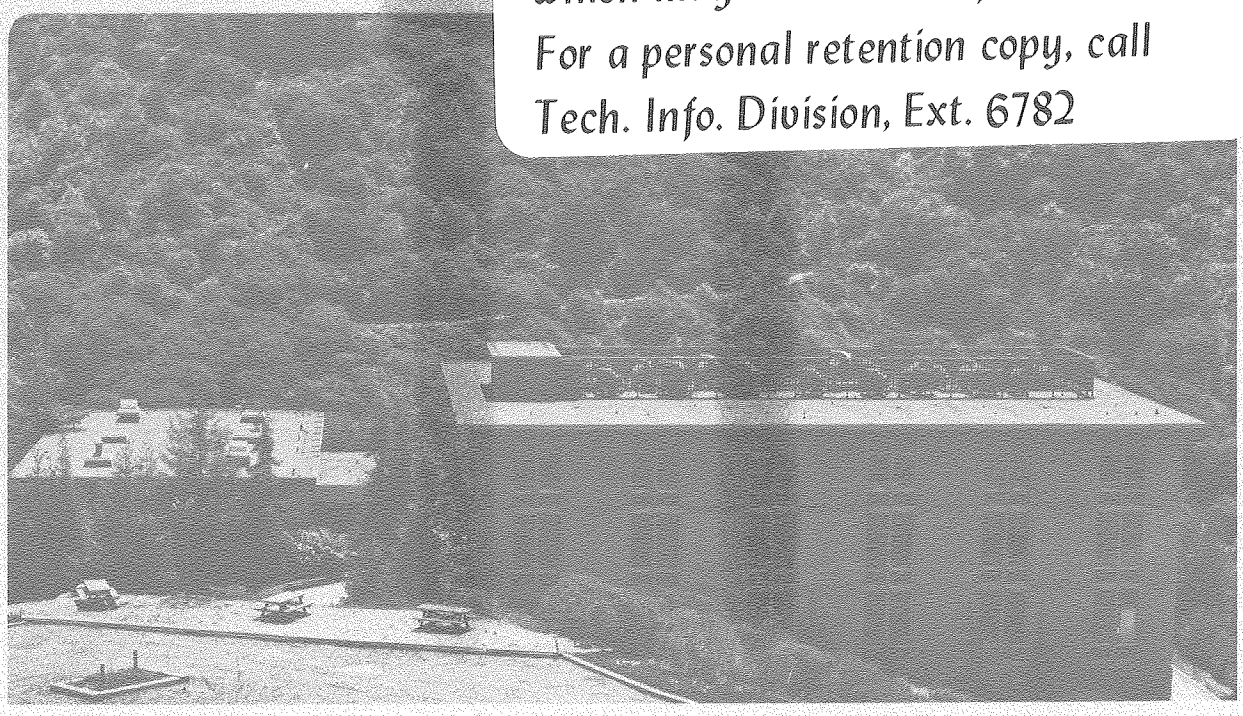

Prepared for the U.S. Department of Energy under Contract W-7405-ENG-48

DISCLAIMER

EFFECT OF VANADIUM ON STRUCTURE-PROPERTY RELATIONS OF DUAL PHASE Fe/Mn/Si/0.1C STEELS

Alvin Nakagawa, J.Y. Koo†, and G. Thomas
Lawrence Berkeley Laboratory
University of California
Department of Materials Science and Mineral Engineering
Berkeley, California 94720

ABSTRACT

The role of vanadium on the structure-property relations of dual phase Fe/Mn/Si/0.1C steels has been investigated. After intercritical annealing at 800°C, the steels with and without V were either iced brine quenched or air cooled. The steels were also solution treated at 900°C and subsequently air cooled. Although V modified the resultant microstructure, especially the morphology of carbides, the corresponding mechanical properties are not significantly affected by the modified microstructures.

It is concluded that V is not beneficial to such dual phase low carbon steels.

I. INTRODUCTION

Significant advances have been made in the past several years in our understanding of structure-property relations in intercritically annealed dual phase steels. Many of the results are published in two recent symposia[1,2]. Among the variables which may be important in influencing these relationships are the volume fraction of martensite, size and distribution of martensite, properties of constituent phases, retained austenite, and precipitation in the ferrite. It is only recently that very fine carbides (or carbonitrides) of the order of 20Å have been observed in the ferrite region of as-quenched dual phase

steels[3,4]. Important consequences of such carbide precipitation on the mechanical properties of dual phase steels containing Nb and Al have been reported by Thomas and Koo[3]. Krauss and his co-workers[5] observed similar precipitation in the retained ferrite of Nb bearing dual phase steels. It has also been shown that the carbide precipitation can also occur in ferrites of many low carbon steels including 1010 steels if the intercritically annealed steels are fast quenched[3,4,6] to room temperature. The carbide forming elements, if present, can enhance the precipitation rate, and are not required to form carbides[6].

Much disagreement still exists as to the role of vanadium on the structure-property relations of dual phase steels. It is possible that V will affect the carbide precipitation in the ferrite, and modify the substructures through its influence on hardenability. The present investigation is, therefore, aimed at understanding the influence of V on the structure-property relations of intercritically annealed dual phase 0.1C steels. Three different heat treatments were employed to produce various microstructures of the steels with and without vanadium.

II. EXPERIMENTAL PROCEDURE

A. Materials Preparation

The chemical compositions of the alloys used in this investigation are given in Table 1. The alloys were vacuum induction melted in the form of 20 lb. cylindrical ingots. The ingots were homogenized in argon at 1100°C for 24 hours. They were upset and cross-forged at 1100°C to 3" by 1" bars and then hot rolled at 1100°C to approximately 1/8". All of the above treatments were followed by air cooling. Oversized tensile blanks were cut from the flat plate with the tensile axis

parallel to the rolling direction.

B. Heat Treatment

The hot rolled specimens were heat treated in a vertical tube furnace under a flowing argon atmosphere. The specimens were either intercritically annealed in the alpha and gamma phase field at 800°C or in the gamma region at 900°C. After a total holding time of 10 minutes, the specimens were subjected to either an iced brine quench (IBQ) or an air cool (AC). The cooling rates from 800°C for the IBQ and AC treatments were approximately 1000°C/sec and 3°C/sec respectively. The cooling rates from 900°C were found to be in the same range. When the alloys were held at 800°C for 10 minutes, the microstructures consisted of about 20% austenite and 80% ferrite.

C. Mechanical Testing

The room temperature tensile properties were determined using 0.1" (2.54 mm) flat tensile bars with 1" (2.54 cm) gauge lengths, according to the ASTM specification E8-69. Approximately 0.8 mm of material was ground from the surface of the specimens to remove any decarburized layers. The decarburization was less than 0.5 mm. Testing was done on an Instron testing machine with a cross-head speed of 0.05 cm/min and a full scale load of 1000 Kg. The total elongations were determined by measuring 1" (2.54 cm) marks on the gauge before and after testing. The rest of the properties were determined from the stress-strain curves produced by the testing machines chart recorder.

D. Microscopy and X-Ray Analysis

The TEM specimens were prepared and observed in the usual way. X-ray diffraction was used to determine the volume fraction of retained austenite in the steels. A solution of 96 ml of 30% H_2O_2 and 4 ml of 40% HF was used to chemically remove 0.8 mm from the surface of the specimen. The resulting shiny surfaces were scanned at 0.2°/min. from $2\theta = 20°$ to $2\theta = 40°$ to include the γ_{200}, α_{200}, γ_{220}, α_{211}, and γ_{311} peaks following the procedure outlined by Miller[7].

III. RESULTS AND DISCUSSION

A. Metallography

Figures 1 through 3 illustrate the optical microstructures developed in the alloys MB and MV after 800 IBQ, 800 AC, and 900 AC heat treatments respectively. General observations indicated that after all three heat treatments the MV alloy had finer grain sizes than those in the MB alloy, presumably due to the role of the undissolved carbides present in the final microstructures of the MV alloy. This was later confirmed by transmission electron microscopy. Another distinct microstructural feature caused by vanadium alloying is the fine precipitates in the ferrite as shown in figures 1 (b), 2 (b), and 3 (b). The nature of these particles was examined by transmission electron microscopy and will be described in a later section. The volume fraction of martensite in the 800 IBQ specimens (figs. 1 (a) and 1 (b)) is about 20%, and that of the second phase in the 800 AC and 900 AC specimens (figs. 2 and 3) is estimated to be about 15%. The vanadium addition does not seem to influence the volume fraction of the second phase to an appreciable extent for any of

the heat treatments investigated here.

The detailed microstructural features of the alloys MB and MV after the three different heat treatments as described earlier were characterized using transmission electron microscopy as follows (see also Table 2).

1. 800 IBQ Microstructures. Transmission electron micrographs from specimens after the 800 IBQ MB treatment are shown in figure 4. Figure 4 (a) reveals an isolated martensite island embedded in the ferrite matrix. Another area showing the martensite/ferrite interface and its vicinity is illustrated in figure 4 (b). It is noted from these representative micrographs that the martensite consists of predominantly dislocated laths and the ferrite region near the interface is heavily dislocated. This feature represents typical microstructures of dual phase steels as reported by many previous investigators[1,2]. The other transformation products of austenite , e.g., bainite and pearlite were not observed in the 800 IBQ MB alloy because of the fast quenching rate employed. Also, there was no evidence of interface precipitation near the martensite/ferrite interfaces. Occasionally, undissolved particles were observed in the transmission electron micrographs, (e.g. fig. 4 (a)), but they were not present in a significant quantity.

The "retained ferrite"[5], the ferrite region retained from the intercritical annealing, showed a fairly extensive precipitation of very fine particles (~ 20Å wide, ~ 100Å long), as shown in figure 4 (c). These particles are presumably carbonitrides[6], and are visible only under favorable diffracting conditions. They have also been observed in many as-quenched dual phase steels, including

1010 steel[6]. It has been shown that the presence of carbide forming alloying elements are not necessary to form precipitates although they may increase the density of precipitation[6].

The microstructures observed in the 800 IBQ MV steel containing V were similar to those of the 800 IBQ MB alloy as described above, except for the marked difference in the interface precipitation in the ferrite near the martensite/ferrite boundaries. The morphology of the carbide precipitation is shown in figure 5 (a). The precise identification of the particles was not attempted in this study, but they are presumably cementite[5,8], or a vanadium carbide[9,10]. The occurrence of the aligned, discontinuous carbides was also observed in dual phase 1010 steel[8] and Nb containing steel[5], and results from the $\gamma \rightarrow \alpha$ + carbide reaction after the completion of the nucleation and growth of "new" proeutectoid ferrite upon quenching. This type of structure is similar to the new eutectoid transformation products observed in the isothermal decomposition of austenite in steels containing strong carbide forming elements[9,10].

A schematic sketch illustrating the sequence of interface precipitation is shown in figure 6. During quenching from the intercritical annealing temperature, the "new" ferrite nucleates epitaxially[5] at the prior austenite/retained ferrite interface and grows until the moving interface is saturated with respect to carbon (or vanadium) to a critical level above which carbides nucleate along the moving interface. The zone of the localized carbides was 1 to 5 μm wide. The particle size is in general coarser in the earlier stage of the

precipitation due to higher transformation temperature, as evidenced by the previous report[8]. Occasionally, the martensitic transformation proceeds before the nucleation of the interface carbides start. As a result, the new ferrite is sandwiched between martensite and retained ferrite, leaving "precipitate free zones". This is shown in figure 5 (b). Very fine carbides (or carbonitrides) are also seen in the retained ferrite, and the density was observed to be higher in this steel than that in the MB alloy. These particles show dislocation loop contrast which is typical of coherent precipitates. It is interesting to note that the mobile dislocations resulting from the $\gamma \rightarrow$ martensite transformation strain are largely concentrated in the new ferrite because this is softer than the particle strengthened retained ferrite phase. The globular, undissolved particles in the V containing steel, as seen in figure 5, showed higher density than those in the MB alloy. This TEM observation appears to be consistent with the optical metallographic examinations.

In summary, the 800 IBQ MV alloy has a narrow zone of discontinuous precipitation of carbides near the martensite/ferrite interface whereas the 800 IBQ MB alloy does not. It appears that V enhances the formation of such carbides even under the severe quenching rate used in this heat treatment.

2. 800 AC Microstructures. The microstructures after air cooling from the 800°C intercritical annealing temperature consisted of ferrite and pearlite in both alloys. Recognizing the complexity of the second phase and the occasional ambiguous distinction between upper

bainite and degenerate pearlite, the second phase may be a mixture of pearlite and upper bainite. There was, however, no evidence of martensite or lower bainite present in the 800 AC specimens. Figure 7 shows a transmission electron micrograph taken from the 800 AC MB alloy. Very few fine carbides were present in either the retained or new ferrite. This result indicates that, upon air cooling, the high carbon content in the retained ferrite at the intercritical annealing temperature partially diffuses into the shrinking austenite. On the other hand, the retained ferrite in the MV alloy showed a relatively higher density of carbide precipitation than that in the MB alloy, but not as high as that observed in the 800 IBQ MV steel. In addition, the interface precipitation type carbides were present in the new ferrite, and their morphology was similar to that observed in the 900 AC MV steel (fig. 8 (b)).

3. 900 AC Microstructures. The final microstructure of the MB alloy after 900 AC treatment was very similar to that of the 800 AC treatment, namely, a mixture of ferrite and pearlite (or upper bainite). The only difference may be that the ferrite in this case is all new ferrite and consequently its carbon content may be slightly different compared to that in the retained ferrite of the 800 AC microstructure. In contrast, the 900 AC MV alloy showed a significant difference in its microstructural constituents. These are shown in figure 8. Approximately 20% of the second phase was martensite probably due to the increased hardenability in the presence of V. The influence of the small addition of V on the improved hardenability was apparently significant enough to cause partial martensitic transformations

in spite of the undissolved vanadium carbides which still remained after 900°C annealing. This result, in comparison with the earlier observation that the 800 AC MV steel did not contain martensite, indicates that more vanadium carbides dissolve after 900°C than 800°C annealing. The result is of course a higher hardenability. The substructure of the martensite was predominantly twinned martensite as shown in figure 8 (a).

Figure 8 (b) illustrates another distinct microstructural feature observed in the 900 AC MV steel. It is seen from figure 8 (b) that there are extremely fine (~ 20 Å), globular particles present in the ferrite in the typical interface alignment morphology. The particles were concentrated in the vicinity of the pearlite or martensite/ferrite interface, and were similar to those observed in the 800 IBQ MV alloy. The relatively coarse and irregular shaped particles which are also seen in the ferrite region of figure 8 (b) appear to be artifacts.

4. Retained Austenite. It has been reported by earlier investigators that the small quantity (~ 5%) of retained austenite is present in the slowly cooled dual phase steels[11,13], especially those containing carbide forming elements. The retained austenite stabilized at room temperature was believed to exist in the form of small equiaxed islands rather than thin films typically observed in the lath martensitic structures[14]. In the present investigation, extensive efforts were made to detect the presence of austenite in the various microstructures examined, but careful X-ray analysis and transmission electron microscopy did not reveal any retained austenite. Thus, if any is

present, it must be less than ~ 1%.

B. Mechanical Properties. The room temperature tensile data are summarized in Table 3, and plotted in figures 9-11. It may be concluded from these data that vanadium does not provide any appreciable improvement in the tensile properties of the base steel for all the heat treatments employed in this study.

For the 800 IBQ treatment, the MB alloy shows even superior tensile properties to the MV alloy, as is seen from Table 3, and also from the stress-strain curve (fig. 9). A plausible explanation can be offered to understand the observed behavior. The MV alloy (0.1%C) can have lower strength than the MB alloy (0.12%C) partly due to the lower initial carbon content, the higher amount of undissolved carbides, and the presence of the undesirable discontinuous carbides near the interface which can act as void nucleation sites upon deformation. At the same time, the strength increment expected from the higher density of fine carbides in the retained ferrite may not be sufficient to balance the decrease in strength caused by the factors listed above.

The stress-strain characteristics of the two steels after the 800 AC and 900 AC heat treatments are illustrated in figures 10 and 11, respectively. Both steels reveal yield point elongation phenomena. In the case of the 800 AC treatment, the MV alloy has about 10 ksi higher yield strength than that of the MB alloy, presumably due to relatively higher density of fine precipitates in the ferrite as discussed earlier. As for the 900 AC treatment, the lower yield strength of the MV alloy compared to that of MB alloy may be due to the residual

stresses introduced by the martensitic transformation observed in the alloy. Thus, it appears that the partial replacement of pearlite with martensite in the 900 AC MV structure only affects the yield strength. This may be partly due to the brittle nature of twinned martensite as opposed to the strong and tough dislocated lath martensite[15].

Due to the complex nature of the microstructures, the coexistence of multiphases, and their inhomogeneous distribution, it is difficult to derive a one-to-one correspondence between microstructure and corresponding mechanical property. However, the results of the present investigation clearly indicate that, although V modifies the microstructural features of the base steel to a significant extent depending on the specific heat treatment, the modified microstructures do not result in the improved mechanical properties for the steel composition and heat treatments considered. The obvious conclusion is that vanadium is not beneficial to such dual phase low carbon steels.

IV. CONCLUSIONS

Based on the present investigation of the effect of V on the structure-property relations of dual phase Fe/Mn/Si/0.1C steels, the following conclusions are drawn.

1. Vanadium refines grain size, enhances fine precipitation in the retained ferrite, and causes discontinuous precipitation to occur in the vicinity of the ferrite/second phase interface. The V addition also increases the hardenability to a significant extent in the case of the 900 AC treatment.

2. The modified microstructures in the presence of V do not improve the mechanical properties for the steel composition and heat treatments considered. Thus, a vanadium addition is not beneficial to such dual phase low carbon steels.

ACKNOWLEDGEMENTS

We are grateful to Foote Mineral Company who supplied the alloys used in this investigation. This work was supported jointly by the Division of Materials Sciences, Office of Basic Energy Sciences, U.S. Department of Energy under contract number W-7405-Eng-48, and Exxon Research and Engineering.

† Corporate Research Science Laboratory, Exxon Research and Engineering Company, Linden, NJ 07036

TABLE 1. Compositions of Steels

ALLOY CODE	CHEMICAL COMPOSITION, WT.%							
	C	Mn	Si	P	S	Al	N	V
MB	0.1	1.15	0.59	0.007	0.003	0.034	0.0097	< 0.01
MV	0.12	1.22	0.62	0.007	0.003	0.039	0.0084	0.12

TABLE 2.

Heat Treatment	Alloy	Second Phase	Interface Precipitation	Fine Precipitation in α	Type of α
800 IBQ	MB	Martensite	No	High	Retained α (and new α)
	MV	Martensite	Yes (extensive)	Very high	Retained α and new α
	MB	Pearlite (upper bainite)	No	Very low	Retained α and new α
	MV	Pearlite (upper bainite)	Yes	Low	Retained α and new α
	MB	Pearlite (upper bainite)	No	Very low	New α
	MV	80% Pearlite (upper bainite) 20% martensite	yes	Medium	New α

TABLE 3. Tensile Properties

Heat Treatment	Alloy	Y.S. ksi	Y.S. MPa	UTS ksi	UTS MPa	Uniform Elongation (%)	Total Elongation (%)
800°C IBQ	MB	65	448	114	785	13	19
	MV	58	400	105	723	13	19
800°C AC	MB	50	345	77	531	17	29
	MV	58	396	75	517	17	29
900°C AC	MB	54	370	75	517	21	35
	MV	50	341	76	520	21	34

REFERENCES

1. Formable HSLA and Dual Phase Steels, Proceedings of the AIME, A.T. Davenport, ed., New York, NY (1979).
2. Structure and Properties of Dual Phase Steels, Proceedings of AIME, R.A. Kot and J.W. Morris, eds., New Orleans, LA (1979).
3. G. Thomas and J.Y. Koo, Structure and Properties of Dual Phase Steels, Proceedings of AIME, R.A. Kot and J.W. Morris, eds., p. 183 (1979).
4. T. O'Neill, M.S. Thesis, University of California, Berkeley, CA, LBL Report # 9047 (1979).
5. M.D. Geib, D.K. Matlock, and G. Krauss, Met. Trans., 11A, p. 1683 (1980).
6. T. O'Neill, J.Y. Koo, and G. Thomas, submitted to Met. Trans. A (1980).
7. R.L. Miller, Trans. ASM, 57, p. 892 (1964).
8. J.Y. Koo and G. Thomas, Mat. Sci. and Engr., 24, p. 187 (1976).
9. R.W.K. Honeycombe, Met. Trans., 7A, p. 915 (1976).
10. A.T. Davenport and P.C. Becker, Met. Trans., 2A, p. 2962, (1971).
11. J.M. Rigsbee and P.J. VanderArend, Formable HSLA and Dual Phase Steels, Proceedings of AIME, A.T. Davenport, ed., P. 56, New York, NY (1979).
12. A.R. Marder, ibid, p. 87.
13. A.P. Coldren, G. Tither, A. Cornford, and J.R. Hiam, ibid, p. 205.

14. B.V.N. Rao, J.Y. Koo, and G. Thomas, Proceedings of the Electron Microscopy Society of America, G.W. Bailey, ed., Claitor's Publishing Company, p. 30 (1975).

15. G. Thomas, Battelle Conference on the Fundamental Aspects of Structural Alloy Design, R.J. Jaffee and B.A. Wilcox, eds., Plenum Press, p. 331 (1977).

FIGURE CAPTIONS

Figure 1. Optical micrographs of the dual phase microstructures developed in the 800 IBQ specimens.
(a) MB alloy (b) MV alloy Nital etch

Figure 2. Optical micrographs of the microstructures observed in the 800 AC specimens.
(a) MB alloy (b) MV alloy Nital etch

Figure 3. Optical micrographs of the microstructures developed in the 900 AC specimens.
(a) MB alloy (b) MV alloy Nital etch

Figure 4. Transmission electron micrographs showing (a) and (b) the structure and morphology of the martensite and ferrite, and (c) the fine precipitates in the retained ferrite region.

Figure 5. Transmission electron micrographs taken from the 800 IBQ MV specimens, showing (a) martensite and discontinuous precipitation in the new ferrite region, and (b) martensite, precipitate free zone, and precipitates in the retained ferrite.

Figure 6. Schematic sketch illustrating the transformation of austenite after intercritical annealing treatment.

Figure 7. Transmission electron micrographs showing both pearlite and ferrite regions. 800 AC MB alloy

Figure 8. Transmission electron micrographs showing (a) twinned martensite embedded in the ferrite matrix, and (b) pearlite and interface type fine carbides in the retained ferrite.

Figure 9. Effect of vanadium on the stress strain curves for 800 IBQ treatment.

Figure 10. Effect of vanadium on the stress strain curves for the 800 AC treatment.

Figure 11. Effect of vanadium on the stress strain curves for the 900 AC treatment.

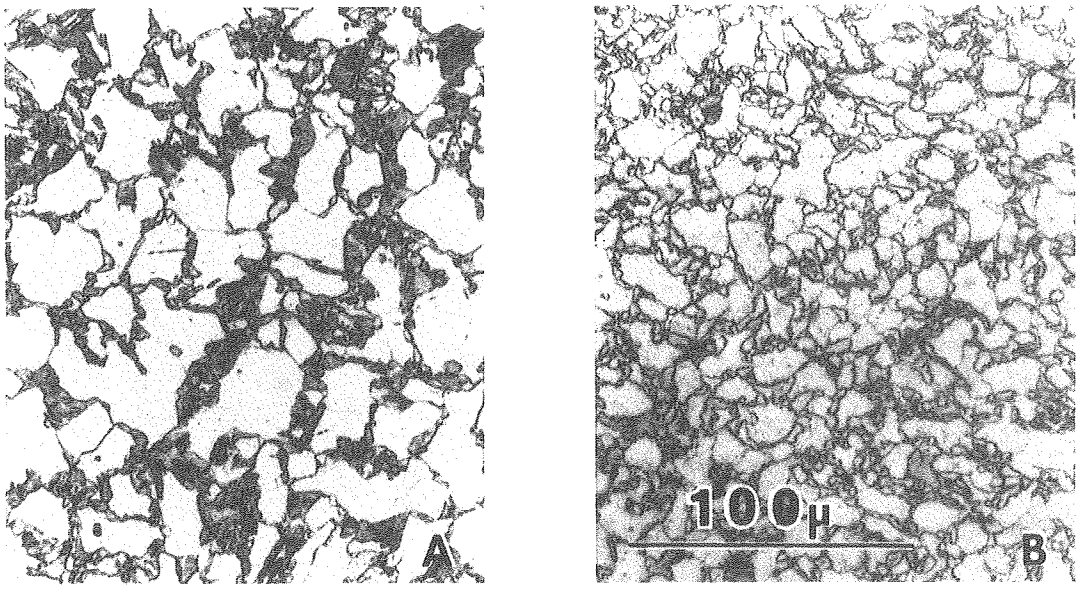

XBB 800-12384

Fig. 1

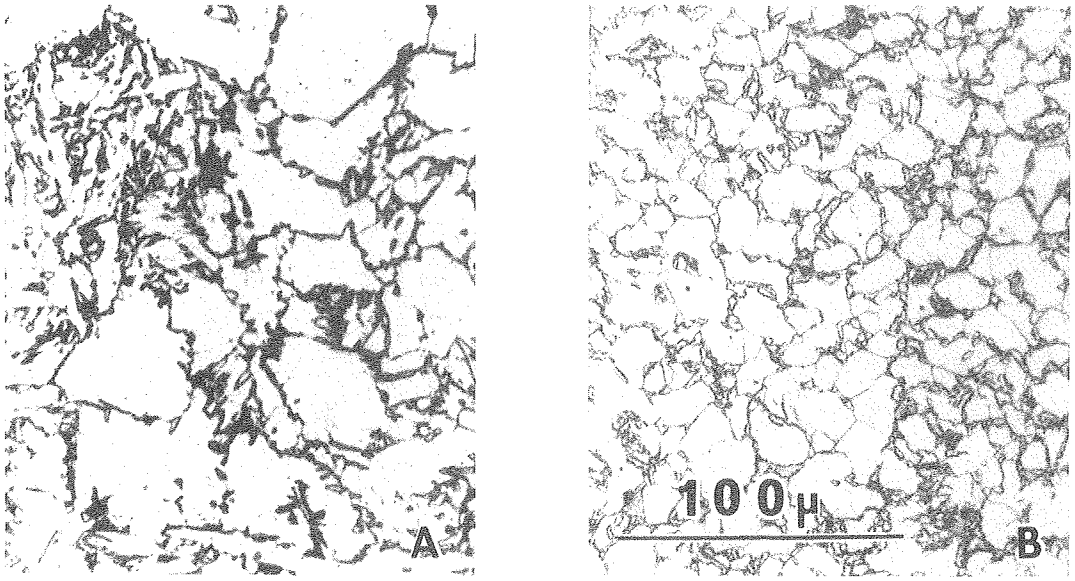

XBB 800-12385

Fig. 2

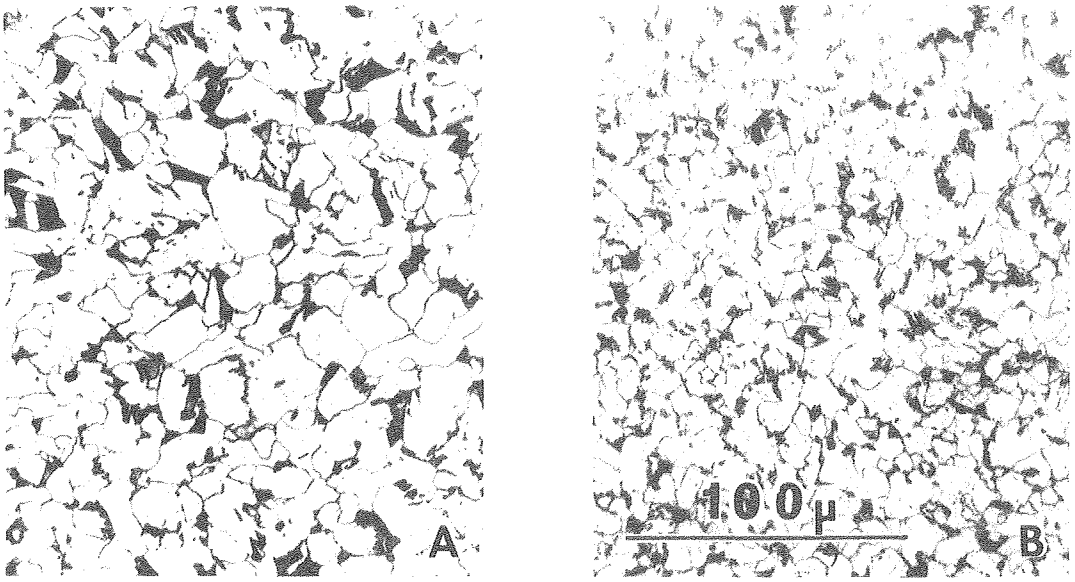

XBB 800-12383

Fig. 3

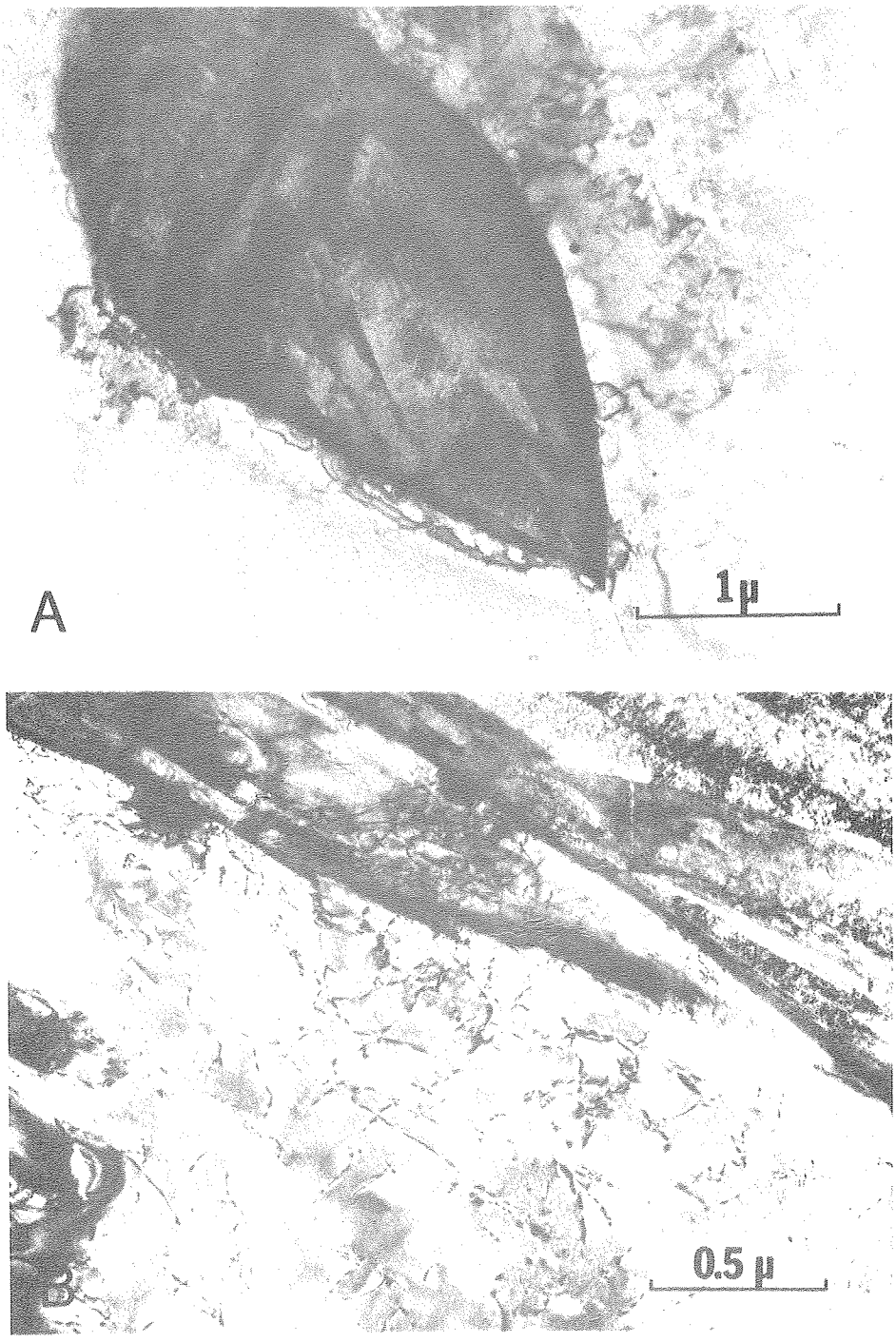

XBB 800-13925

Figs. 4 a and b

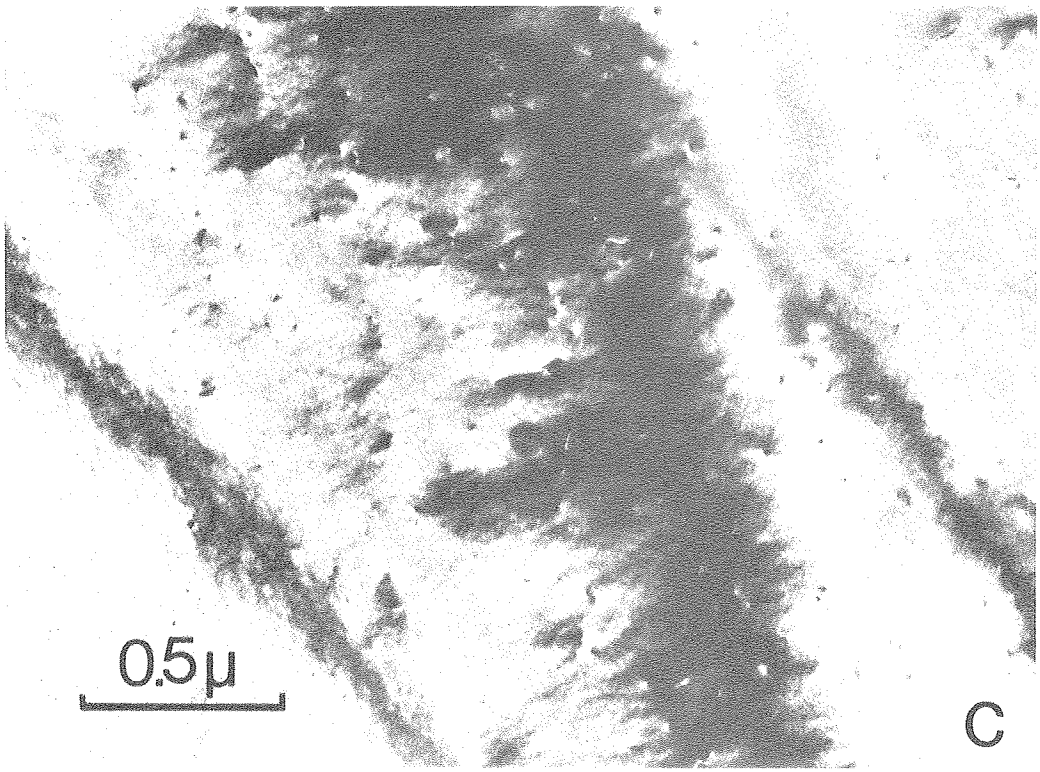

XBB 800-12392

Fig. 4c

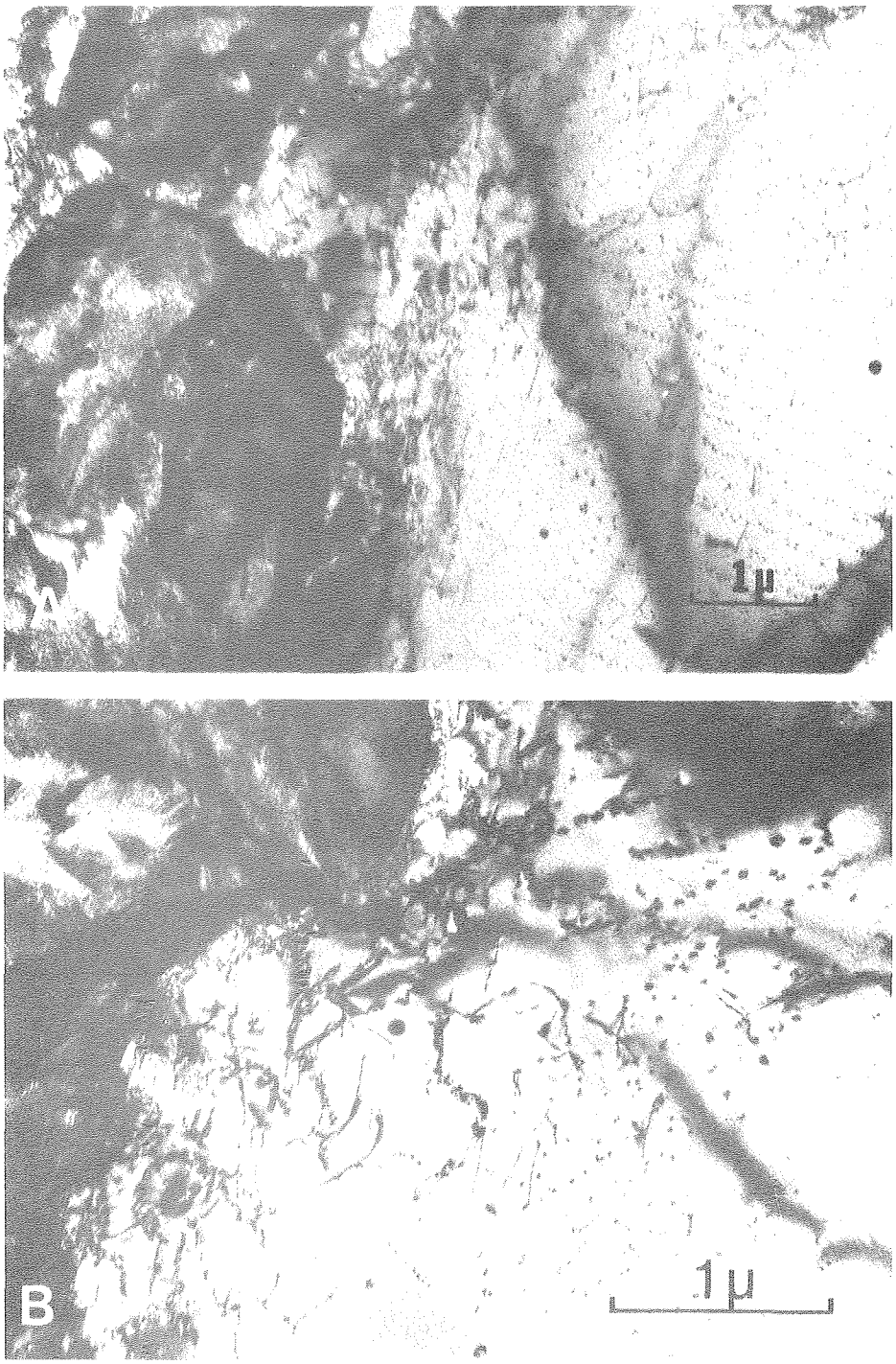

XBB 800-13924

Fig. 5 a and b

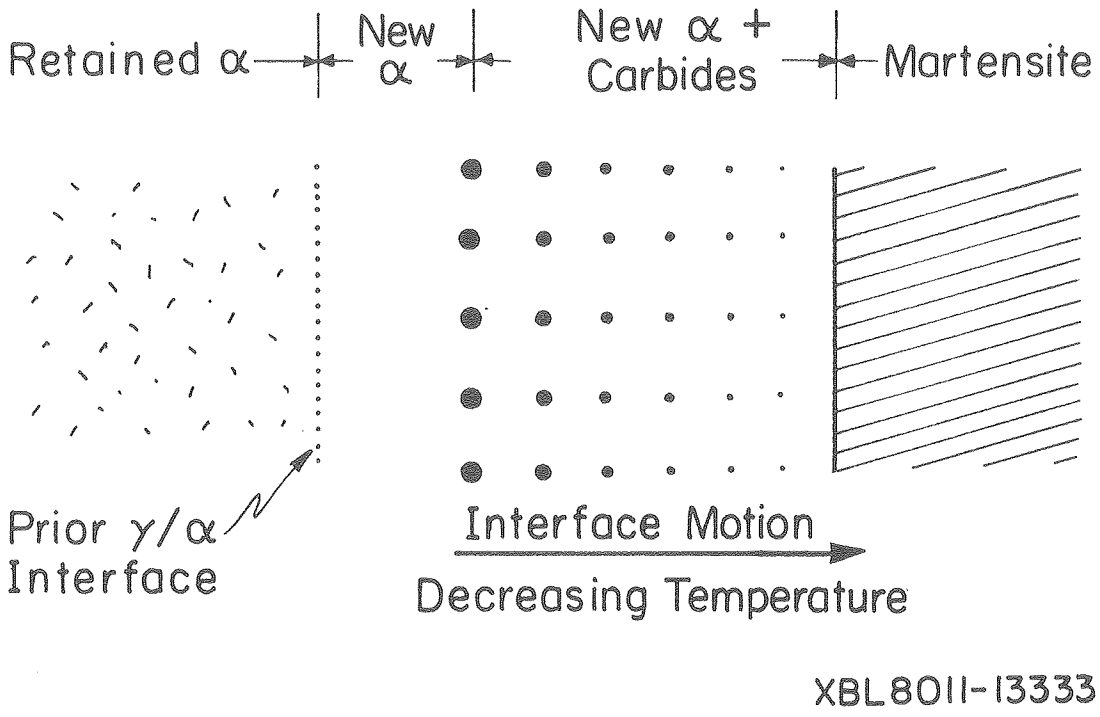
Retained α
New α
New α + Carbides
Martensite
Prior γ/α Interface
Interface Motion
Decreasing Temperature
XBL8011-13333

Fig. 6

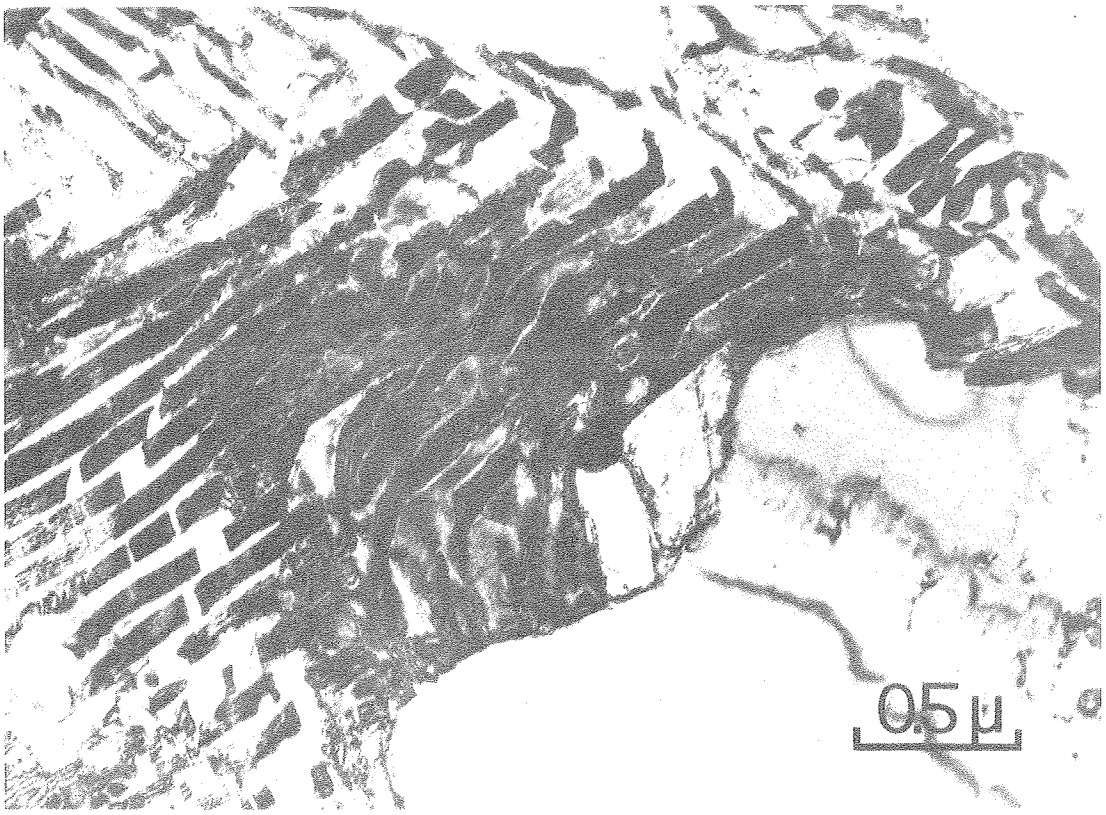

XBB 800-13923

Fig. 7

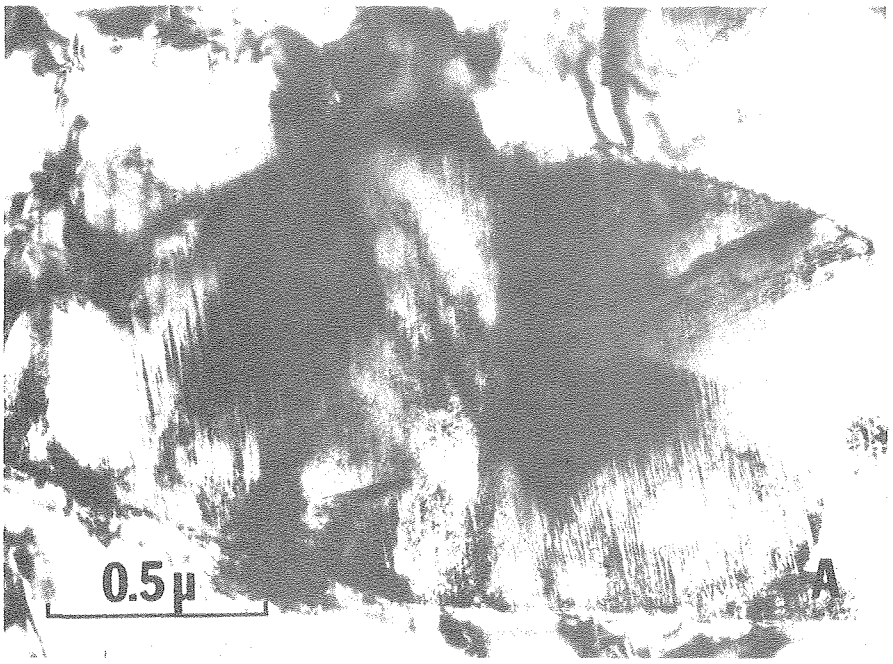

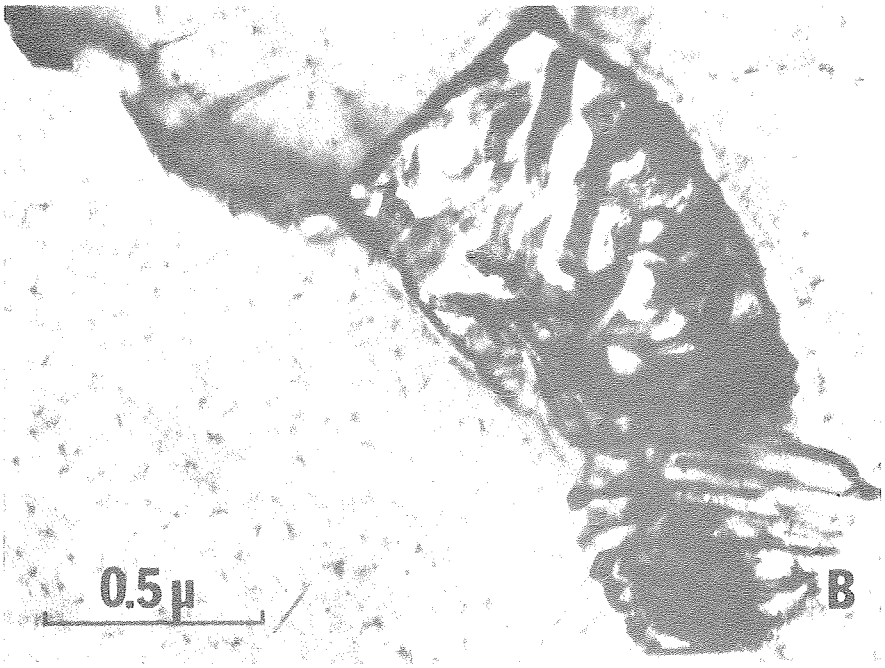

XBB 811-53

Fig. 8 a and b

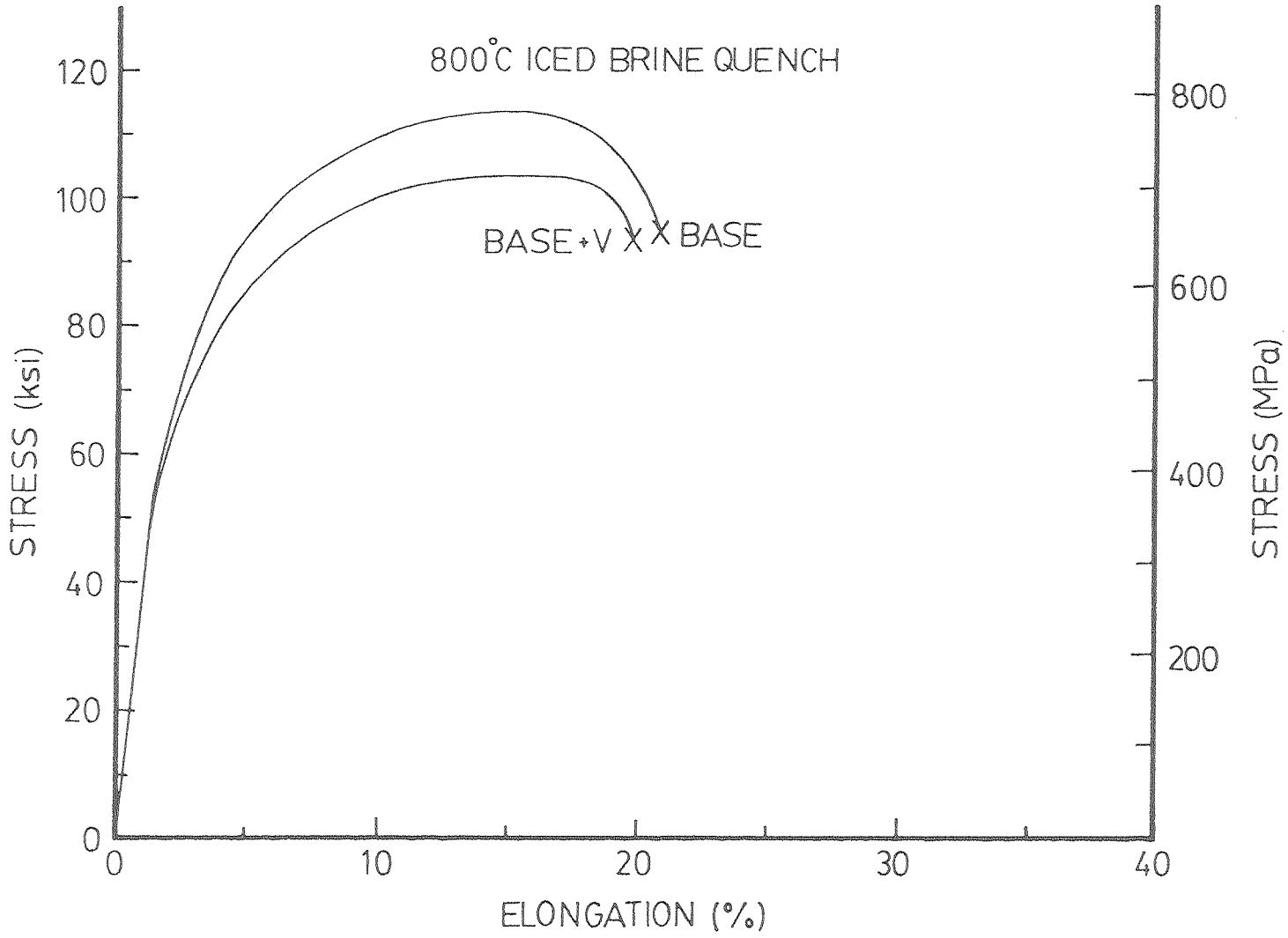

XBL 8011-7408

Fig. 9

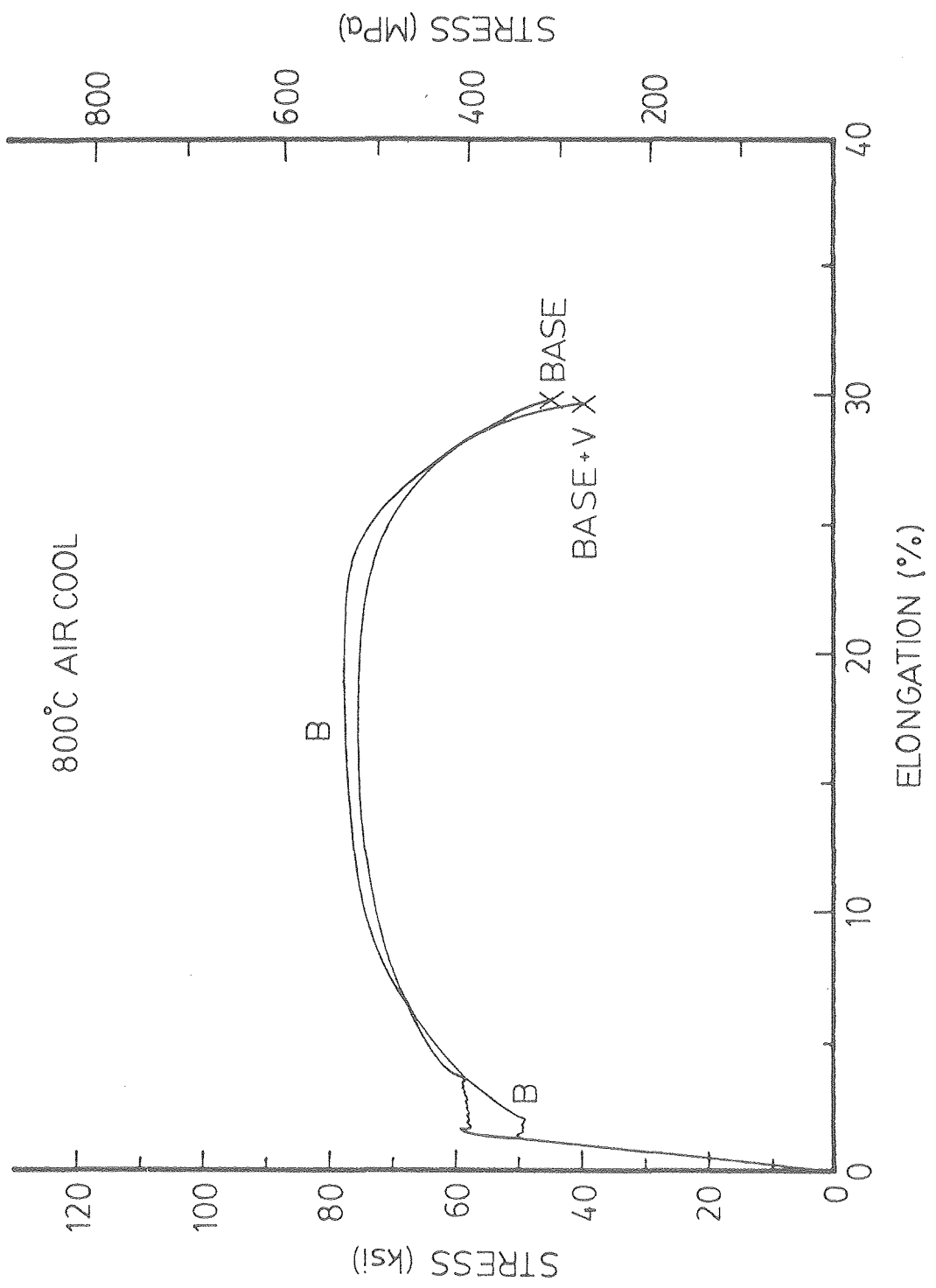

XBL 8011-7407

Fig. 10

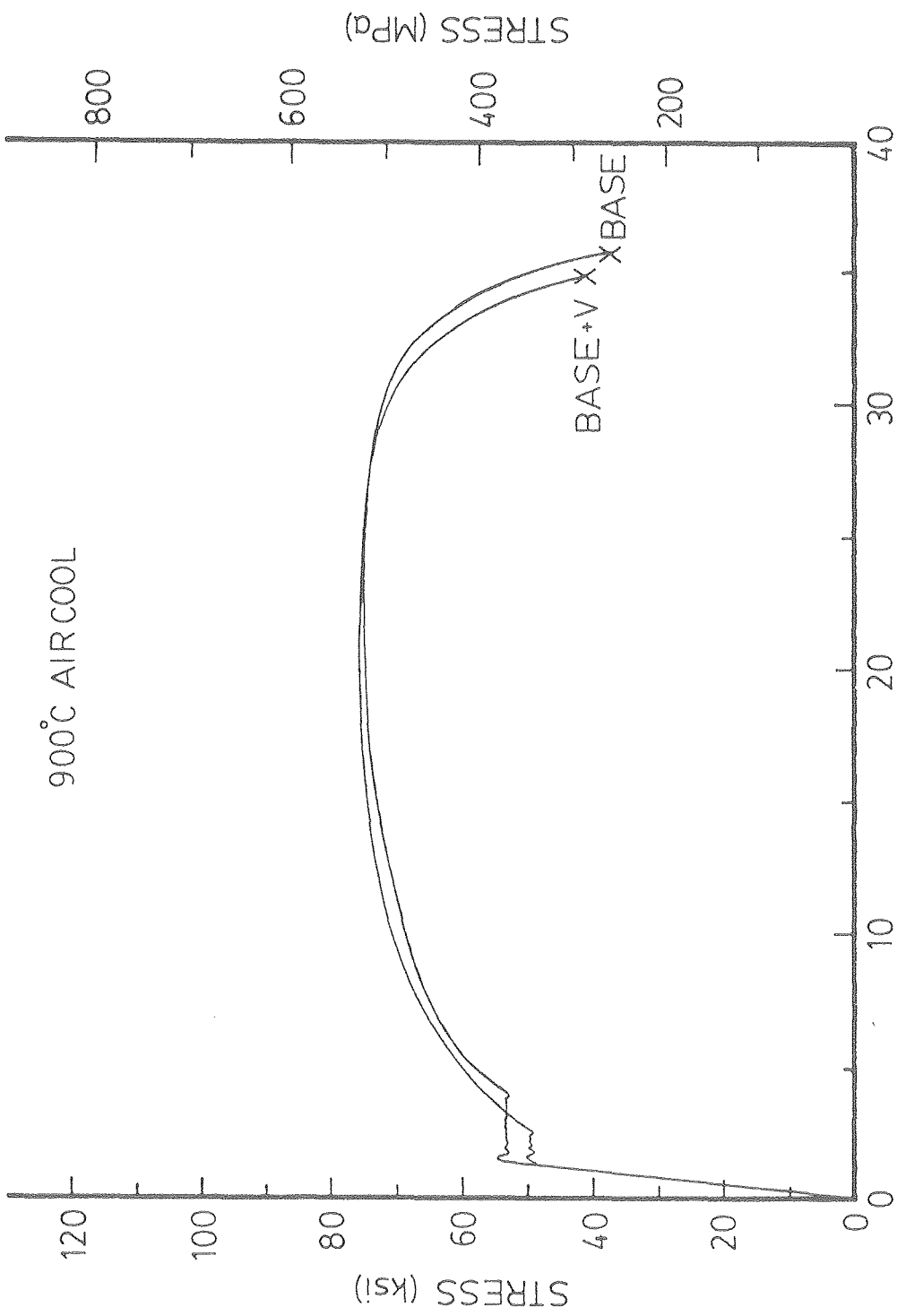

XBL 8011-7410

Fig. 11